

Population Pharmacokinetics of CC-122

Yiming Cheng¹Jian Chen²Michael Pourdehnad ³Simon Zhou¹Yan Li¹¹Clinical Pharmacology & Pharmacometrics, Bristol Myers Squibb, Summit, NJ, USA;²Non-Clinical Research & Development, Bristol Myers Squibb, Summit, NJ, USA;³Early Clinical Development, Bristol Myers Squibb, San Francisco, CA, USA

Background: CC-122 is a cereblon-modulating agent that exerts direct cell-autonomous activity against malignant B cells and immunomodulatory effects. Herein, a population pharmacokinetic (popPK) model of CC-122 was developed and the influence of demographic and disease-related covariates on population pharmacokinetic parameters was assessed based on data from three clinical studies of CC-122 (dose range, 0.5–15 mg) in healthy subjects and cancer patients.

Methods: Nonlinear mixed effects modeling was employed in developing a population pharmacokinetic model of CC-122 based on 298 patients from 3 clinical studies.

Results: The PK of CC-122 was adequately described with a two-compartment model with first-order absorption and elimination. Tumor types were found to be significantly correlated with apparent clearance (CL/F) and apparent volume of distribution of the central compartment. Creatinine clearance was identified as a statistically significant covariate of CL/F. Sex and body weight were statistically but not clinically relevant on V2/F.

Conclusion: In conclusion, the two-compartment model built can be used to adequately describe the time course of the population pharmacokinetics of CC-122 and should serve as the basis for dose adjustment decision-making of CC-122.

Keywords: CC-122, population pharmacokinetics, renal impairment

Introduction

CC-122 is a cereblon-modulating agent that exerts direct cell-autonomous activity against malignant B cells and immunomodulatory effects. Based on *in vitro* studies, CC-122 exhibited multiple pharmacological activities, including antiproliferative activity in diffuse large B cell lymphoma (DLBCL), mantle cell lymphoma (MCL), follicular lymphoma (FL), chronic lymphocytic leukemia (CLL), and multiple myeloma (MM) represented by multiple cell lines, antigrowth activity in hepatocellular carcinoma (HCC), and antiangiogenic activity by inhibition of endothelial cell sprout formation, growth factor induced endothelial cell migration and invasion, and hypoxia-inducible factor (HIF)-1 α protein expression *in vitro*. The anti-tumor activity of CC-122 was also shown in xenograft models of human myeloma, glioblastoma, and human lymphoma.^{1–3} Based on its antiproliferative and antitumor activities, CC-122 is being investigated as an oncology treatment for non-Hodgkin lymphoma (NHL), including DLBCL and FL; CLL; MM; and/or advanced solid tumors, including glioblastoma multiforme (GBM) and HCC.^{4–6}

The pharmacokinetics (PK) properties of CC-122 have been characterized in multiple studies. Healthy adult subjects receiving a single oral dose of CC-122 (3 to 15 mg) showed rapid absorption (time to maximum observed plasma concentration, t_{max} approximately 1 hour). The terminal half-life was estimated to be 7.6–8.9 hours.⁷ In a first-in-human study (in patients with cancer), CC-122 exposure

Correspondence: Yan Li
Clinical Pharmacology & Pharmacometrics,
Bristol Myers Squibb, 556 Morris Ave,
Summit, NJ, 07901, USA
Tel +1 908-481-6203
Email yan.li@bms.com

increased in a dose-dependent manner from 0.5 to 3.5 mg.⁴ A dedicated human [¹⁴C]-label study evaluating the metabolism and excretion of CC-122 showed that parent CC-122 was the predominant circulating component in plasma and urine excretion was one of the major elimination routes (data on file). In vitro study indicated that cytochrome P450 (CYP) 3A and CYP1A2 appear to be the major enzymes involved in the oxidative metabolism of CC-122. Based on the metabolic profile, Ogasawara et al assessed the drug–drug interaction potential of CC-122 when co-administered with CYP1A2 and CYP3A modulators.⁸ In a recent publication from an open-label, single-dose study to evaluate the impact of renal impairment on CC-122 pharmacokinetic disposition, Li et al reported that following administration of a single oral dose of 3 mg CC-122, renal impairment reduced both the apparent total plasma clearance and renal clearance of CC-122.⁹

In this article, a population PK model was developed to characterize CC-122 concentration–time profiles in healthy subjects and patients with advanced solid tumors and hematological malignancies. In addition, the effects of subject characteristics on CC-122 PK were investigated.

Materials and Methods

Clinical Study Data

Subjects from studies CC-122-CP-002 (Part 1), CC-122-CP-005 and CC-122-ST-001 (NCT01421524) were included in population PK analyses. Study CC-122-CP-002 part 1 was a Phase I study to evaluate safety, tolerability, and PK of CC-122 following single oral doses in healthy adult subjects. Study CC-122-CP-005 was a phase I, open-label, single-dose study to assess the pharmacokinetics of CC-122 in subjects with mild, moderate, and severe renal impairment and matched healthy subjects. CC-122-ST-001 was a phase 1a/b, open-label, dose-finding study to assess safety, tolerability, PK, and preliminary efficacy of CC-122 in advanced solid tumors, NHL, MM, or advanced unresectable solid tumors, including in patients who have progressed on (or cannot tolerate) standard therapy or for whom no standard anticancer therapy exists.

The studies were conducted in accordance with the ethical principles of Good Clinical Practice. All subjects gave written informed consent prior to enrollment. The studies were approved by the institutional review boards ([Supplementary Table 1](#)) of the participating center and

were conducted according to the Declaration of Helsinki and the ICH Guidelines for Good Clinical Practice.

Bioanalytical Methods

CC-122 is a chiral racemic mix of its enantiomers (S-CC-122 and R-CC-122). Both achiral method (used in CC-122-CP-002 and CC-122-CP-005 studies) and chiral method (used in CC-122-ST-001 study) were validated to determine the concentrations of CC-122 or its R and S enantiomers in K3EDTA human plasma utilizing liquid chromatography–tandem mass spectrometry (LC-MS/MS) technology. Human plasma samples were spiked with stable ¹³C-labeled CC-122 as an internal standard (IS). CC-122 and [¹³C5]-CC-122 (IS) were then extracted by solid phase extraction using a Tomtec Quadra 4 SPE system with Waters Oasis μ -Elution HLB plate (30 μ m). CC-122 and [¹³C5]-CC-122 from plasma samples were eluted from HLB plate with ACN:H₂O:formic acid/25:75:0.1 (v:v:v). For achiral assay, the samples were injected for LC–MS/MS analysis using a Phenomenex Synergi Polar-RP analytical column (80Å, 50×2.0 mm, 4 μ m) and mobile phases of A (0.1% formic acid in H₂O) and B (0.1% formic acid in acetonitrile). For chiral assay, the samples were injected for LC–MS/MS on a Phenomenex Synergi Polar-RP analytical column (80Å, 30×2.0 mm, 4 μ m) coupled with a ChiralTech Chiral-AGP (150×3.0 mm, 5 μ m) and mobile phases of A (10mM ammonium formate with 0.005% acetic acid in water) and B (Methanol). Positive ions were measured in the multiple reaction monitoring (MRM) mode ($m/z = 287.1 \rightarrow 176.1$ for CC-122 and its enantiomers and $m/z = 292.1 \rightarrow 176.1$ for IS and its enantiomers) using an API 4000 or AB Sciex QTRAP 5500 tandem mass spectrometer equipped with a TurboIonSpray source. The lower limit of quantification (LLOQ) were 1.0 ng/mL for CC-122 and 0.5 ng/mL for R-CC-122 and S-CC-122. The calibration ranges were 1.0 to 400.0 ng/mL for achiral assay and 0.5 to 200.0 ng/mL for chiral assay.

Structural Population Pharmacokinetic Model

The population PK analysis was conducted using NONMEM Version 7.3 with the first-order conditional estimation (FOCE) (ICON Development Solutions, Ellicott City, MD). Perl-speaks-NONMEM (PsN Version 4.6.0) was used to assess the PK model and the results were further analyzed by R (Version 3.5.1).

As a starting point, prior knowledge of CC-122 disposition and graphical examination of the raw data were

leveraged to select the most appropriate model. Accordingly, CC-122 PK was best described by a one- or two-compartment model, as supported by the PK sampling frequency, with first-order absorption and a lag time. Assuming a log-normal distribution for interindividual variability (IIV) in PK parameters, IIV was modeled using an exponential random-effect model to ensure positive PK parameters. Assuming a log-normal distribution of residual variability (RV) in concentration data, additive error models after logarithmically transforming the model predictions were used to describe the residual variability.

Goodness of fit, scientific plausibility, log-likelihood ratio test, and visual predictive check (VPC) plot were used to evaluate the model.

Covariate Analysis

Covariates were incorporated into the model to explain the variabilities of the CC-122 PK. Based on the biological

understanding, the following factors were investigated: age, body mass index (BMI), weight, sex, serum albumin, alanine aminotransferase, aspartate aminotransferase, bilirubin, creatinine clearance and tumor type. Graphical examination for observable trends was used to assist in determining the relationship between the parameter and the covariate (Figure 1).

The median (continuous) or most prevalent (categorical) covariate values were used as the reference population. The stepwise covariate model (SCM) building tool of PsN was employed for development of the CC-122 covariate model, which implemented forward selection ($p < 0.01$) and backward elimination ($p < 0.001$) of covariates for the CC-122 pop PK model and was previously used in other publication.¹⁰ A fixed set of PK parameter-covariate relations is defined in the SCM; predefined shapes for the parameter-covariate relations for continuous covariates include the following:

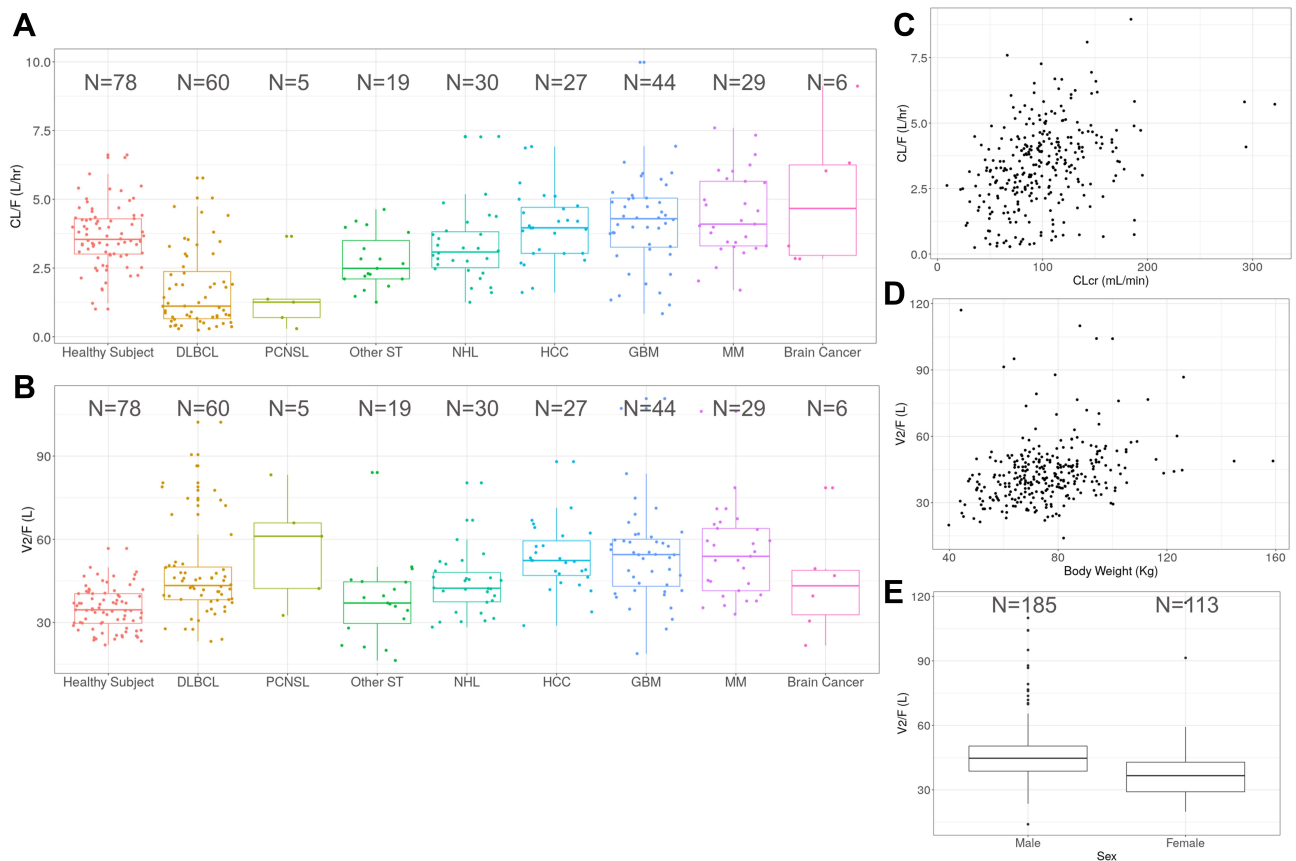


Figure 1 Graphical examinations of observable trends between relevant popPK parameters and covariates. Box plot of apparent clearance (CL/F, **A**) and apparent volume of distribution of the central compartment (V2/F, **B**) of CC-122 by tumor types. **(C)** Scatter plot of apparent clearance (CL/F) vs creatinine clearance (CLcr). **(D)** Scatter plot of apparent volume of distribution of the central compartment (V2/F) vs body weight. **(E)** Box plot of apparent volume of distribution of the central compartment (V2/F) by sex. Individual estimates of CL/F and V2/F were obtained from the base model.

Abbreviations: DLBCL, diffuse large B cell lymphoma; PCNSL, primary CNS lymphoma; other ST, other solid tumor; NHL, non-Hodgkin lymphoma; HCC, hepatocellular carcinoma; GBM, glioblastoma multiforme; MM, multiple myeloma.

$$\text{Linear equation : } P = \theta * (1 + \theta_{cov} * (COV_i - COV_m)) \quad (1)$$

$$\text{Power equation : } P = \theta * \left(\frac{COV_i}{COV_m} \right) * \theta_{cov} \quad (2)$$

where P is the typical value of a PK parameter in the population after adjusting values of covariates individual subject, θ is the typical value of PK parameter, θ_{cov} is the coefficient or the effect of the covariate, COV_i is the covariate value for individual subject, and COV_m is the median value of covariates in the study population.

Categorical covariates were included in the model as below:

$$P = \theta * (1 + \theta_{cov} * Z_{ind,k}) \quad (3)$$

where $Z_{ind,k}$ is an indicator variable representing 1 or 0 from a binary covariate and θ_{cov} is the coefficient for the effect of the covariate.

Model Performance

Nonparametric bootstrap resampling and VPC were used to assess the performance of the final CC-122 pop PK model. To implement the nonparametric bootstrap, firstly, new datasets were created using resampling with replacement. Then, the new datasets were re-fitted to the popPK model and the corresponding parameters were generated for each dataset. One thousand bootstrap replicates were conducted and the median and non-parametric 95% confidence interval (CI) of these parameters were calculated and summarized.

The VPC was used to assess the agreement between observations and model predictions. One thousand simulations using the fixed and random parameters of the model were performed. The 95% prediction intervals for the 5th, 50th, and 95th percentiles of simulated data were compared to the corresponding observed data.

Results

Summary of Analysis Dataset

A total of 298 subjects were included in the final population PK analysis dataset. Demographic characteristics of these subjects are shown in Table 1. The subjects had a median (range) age (years) of 59.5 (20.0–91.0) years and body weight (kg) of 74.5 (39.8–159.0). The median (range) creatinine clearance (CL_{cr}), a marker associated with renal function, was 94.4 (9.0, 321.2) mL/min. And, 73.8% subjects were cancer patients. Eight tumor types were included in the

analyses, including DLBCL (n=60), PCNSL (n=5), NHL (n=30), HCC (n=27), GBM (n=44), MM (n=29), brain cancer (n=6) and other solid tumor (n=19). Among these, DLBCL (20.1%), GBM (14.8%) and NHL (10.1%) were relatively prevalent.

Structural Population Pharmacokinetic Model

A population PK analysis was performed based on rich and sparse plasma concentration data (Figure 2). The two-compartment model with first-order absorption was preferred over the one-compartment model due to better minimization, more reliable parameter estimates and decreasing OFV (ΔOFV : -749). In addition, incorporating a lag time improved the model fitting by significantly decreasing OFV (ΔOFV : -491).

During model development, it was noted that the peripheral compartment volume of distribution (V₃) estimation was primarily dependent upon rich PK samples from healthy subjects (CP-002 and CP-005 studies). When pooled together with patient trial (ST-001), the V₃ information was likely diluted, resulting a high degree of uncertainties (%RSE>100%). Thus, in the final model, V₃ was fixed to 10 L, which was estimated from healthy subjects with good precision (%RSE <30%).

According to goodness-of-fit and statistical criteria, the two-compartment model with first-order absorption and elimination and absorption lag time was selected as the structural model (Figure 3). Log-transformation of concentrations allowed better estimates of parameters and results from the analysis were more stable interindividual variability on apparent clearance (CL/F), apparent central compartment volume of distribution (V₂/F), intercompartment clearance (Q) and first-order absorption rate constant (K_a) were estimated.

Final Pharmacokinetic Model

All proposed covariates were included in covariate model development using the SCM building tool of PsN. The output of SCM-building log file indicated that inclusion of tumor type and CL_{cr} into CL/F and inclusion of tumor type, sex and body weight into V₂/F significantly improved the model fit. A linear equation between V₂/F and body weight values and a linear equation between CL/F and CL_{cr} significantly improved the model fit compared to power equation.

The PK parameters from the final population PK model for CC-122 are presented in Table 2. Most of the PK parameters for the final model were estimated with good

Table I Demographic and Baseline Characteristics of 298 Subjects from CC-122-CP-002, CC-122-CP-005 and CC-122-ST-001 Studies

Subject	Median (Range)				
		CC-122-CP-002	CC-122-CP-005	CC-122-ST-001	Total
Continuous Variables					
Count		30	48	220	298
Age (years)		32.5 (20–60)	58.5 (26–75)	62 (25–91)	59.5 (20.0–91.0)
Height (cm)		171 (158–199)	173 (151–186)	168 (142–193)	168 (142–199)
Weight (kg)		75.8 (52.9–95)	79.1 (57.7–126.0)	73 (39.8–159.0)	74.5 (39.8–159.0)
BMI (kg/m ²)		26.0 (19.3–31.5)	27.3 (19.7–37.1)	25.9 (15.3–54.9)	25.9 (15.3–54.9)
Creatinine clearance (mL/min)		107.0 (76.3–171.0)	90.6 (9.0–152.0)	92.1 (35.3–321.2)	94.4 (9.0–321.2)
Serum albumin (g/L)		45 (40–52)	31 (33–48)	38 (14–42,900)	40 (14–42,900)
Alanine aminotransferase (U/L)		15.0 (8.0–36.0)	15.5 (6.0–46.0)	27.0 (7.0–227.0)	22.0 (6.0–227.0)
Aspartate aminotransferase (U/L)		16.5 (9.0–25.0)	19.0 (7.0–36.0)	25.0 (7.0–205.0)	22.0 (7.0–205.0)
Bilirubin (μmol/L)		9.0 (4.4–18.5)	7.7 (3.4–22.2)	8.6 (1.7–85.5)	8.5 (1.7–85.5)
Categorical Variables		N (%)			
Sex		CC-122-CP-002	CC-122-CP-005	CC-122-ST-001	Total
	Male	25 (83.3)	27 (56.3)	133 (60.5)	185 (62.1)
	Female	5 (16.7)	21 (43.7)	87 (39.5)	113 (37.9)
Tumor	Healthy	78 (26.2)			
	DLBCL	60 (20.1)			
	PCNSL	5 (1.7)			
	Other solid tumor	19 (6.4)			
	NHL	30 (10.1)			
	HCC	27 (9.1)			
	GBM	44 (14.8)			
	MM	29 (9.7)			
	Brain cancer	6 (2.0)			

Abbreviations: DLBCL, diffuse large B cell lymphoma; PCNSL, primary CNS lymphoma; NHL, non-Hodgkin lymphoma; HCC, hepatocellular carcinoma; GBM, glioblastoma multiforme; MM, multiple myeloma.

precision (relatively narrow 95% CI from 1000 bootstrap runs). The final model suggested that CL/F was dependent on tumor type (Table 2; Figure 1A) and CLcr (Table 2; Figure 1C). The CL/F in cancer patients were 34.8% (DLBCL), 30.3% (PCNSL), 89.3% (NHL), 109.2% (HCC), 107.9% (GBM), 120.0% (MM), 131.6% (brain tumor) and 73.7% (other solid tumors) of healthy subjects (Figure 4A). Due to the small CL/F difference in NHL, HCC and GBM cohorts compared with healthy subjects and relatively limited number of patients but large variabilities in brain cancer (n=6) cohort, effects of these tumor types were not incorporated in the model to ensure stability (fix to 0).

CLcr was positively correlated with CL/F, which was described by a linear equation (Table 2). The CL/F in subjects with 60 to 90 mL/hr and less than 60 mL/hr CLcr was 69.3% and 50.2% of the subjects with greater than 90 mL/hr (Figure 4A), respectively, indicating that renal function failure impaired the clearance of CC-122, which was consistent with previous finding.⁹ Due to the

limited number of patients in less than 30 mL/min category (n=5), no further analysis was conducted.

The apparent volume of distribution (V2/F) was associated with tumor types (Figure 1B), body weight (Figure 1D), and sex (Figure 1E). Body weight was positively correlated with V2/F, which was described by a linear equation in the model (Table 2). Male subjects tended to have higher V2/F (26.8% higher) compared to females. Cancer patients consistently showed higher V2/F, with 3.3% to 57.8% increase compared to healthy subjects (Figure 4B). However, due to the small difference (3.3%) in other solid tumor cohort, effect of this tumor type (other solid tumor) was not included in the final model (fix to 0).

In addition, no clinically meaningful effect on the PK of CC-122 was observed including age (20 to 91 years), BMI (15.3 to 54.9 kg/m²), serum albumin (14–42,900 g/L), alanine aminotransferase (6.0 to 227.0 U/L), aspartate aminotransferase (7.0–205.0 U/L) and total bilirubin (1.7–85.5 μmol/L) in the population PK analysis.

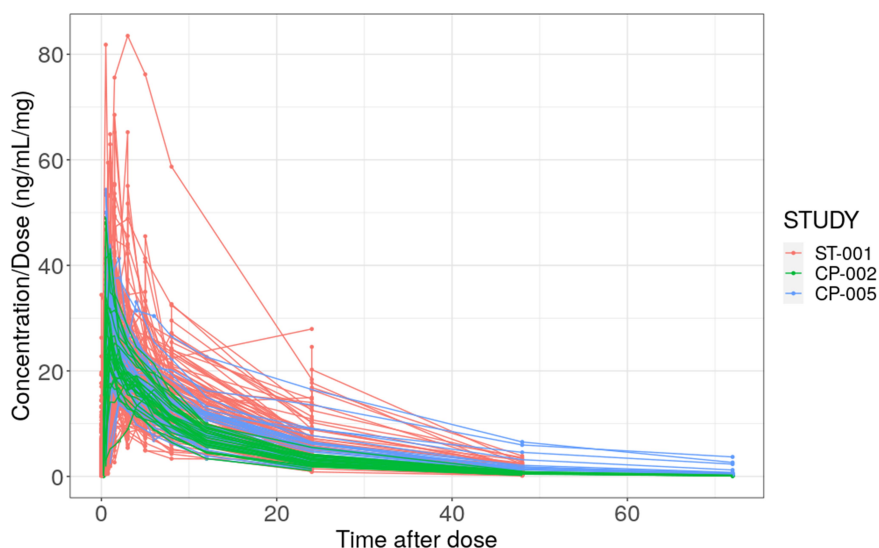


Figure 2 Individual dose-normalized CC-122 concentration vs time profiles by studies. Red: CC-122-ST-001 study; Green: CC-122-CP-002 study; Blue: CC-122-CP-005 study.

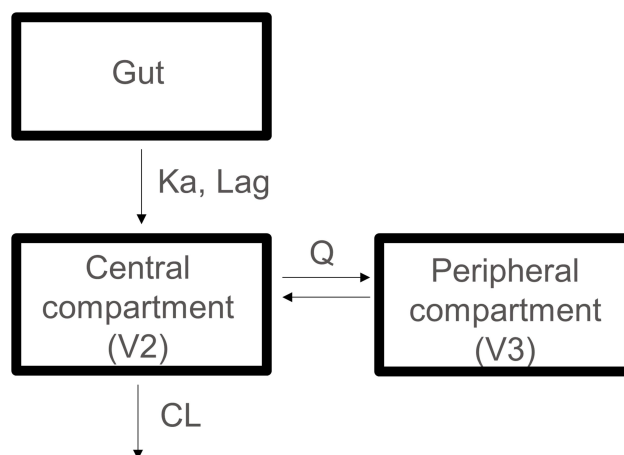


Figure 3 The population pharmacokinetic model of CC-122. The model comprises two-compartment with first-order absorption incorporating a lag time and first-order elimination.

The final population PK model of CC-122 was also evaluated using VPC with 1000 simulations (Figure 5). The 5th, 50th and 95th percentiles of the observed concentration data at each time point were generally contained within the respective 95% CI of the simulated data. There was a good agreement in the time course and central tendency between distributions of observed and simulated concentration data, with no obvious bias. Goodness-of-fit plots indicated that the final model fitted well to the observed data (Figure 6). The distribution of conditional weighted residuals (CWRES) was homogeneously and evenly distributed around zero across the population predicted concentrations or sampling times, suggesting no

obvious bias in the predictions of high and low concentrations of CC-122. Taken together, CC-122 concentrations were well characterized by the final population PK model.

Discussion and Conclusions

CC-122 concentration–time data from doses of 0.5 mg to 15 mg administered daily to healthy subjects (CC-122-CP-002 and CC-122-CP-005) and patients with advanced solid tumors, NHL, MM, or advanced unresectable solid tumors (CC-122-ST-001) were adequately described by a two-compartment model with first-order absorption incorporating a lag time and first-order elimination. Tumor types and CL_{cr} were identified as statistically

Table 2 Population Pharmacokinetic Parameter Estimates of CC-122 from the Final Model

Parameter	Parameter Estimates	RSE%	Bootstrap Median (95% CI) ^a
Fixed Effect			
TVCL/F	3.63	3.5	3.55 (3.24 to 3.82)
TVV2/F	36.2	5.7	36.2 (35.06 to 39.68)
TVQ/F	1.38	49.9	1.38 (1.05 to 1.64)
TVV3/F	10 Fix		10 Fix
TVKa	4.14	20.5	4.14 (3.50 to 5.10)
TVALAG	0.246	0.6	0.246 (0.242 to 0.248)
Tumor type (DLBCL) on CL/F ^b	-0.647	11.3	-0.647 (-0.774 to -0.519)
Tumor type (PCNSL) on CL/F ^b	-0.692	36.7	-0.692 (-0.908 to -0.076)
Tumor type (other solid tumor) on CL/F ^b	-0.364	16.5	-0.364 (-0.438 to -0.251)
Tumor type (MM) on CL/F ^b	0.309	74.8	0.309 (0.051 to 0.650)
CLcr on CL/F ^b	0.007	65	0.007 (0.004 to 0.008)
Body weight on V2/F ^c	0.009	47	0.009 (0.006 to 0.011)
Sex on V2/F ^c	-0.179	41.6	-0.179 (-0.247 to -0.120)
Tumor type (DLBCL) on V2/F ^c	0.476	29.2	0.474 (0.247 to 0.634)
Tumor type (PCNSL) on V2/F ^c	0.846	52.2	0.846 (0.088 to 2.23)
Tumor type (NHL) on V2/F ^c	0.344	38.4	0.344 (0.170 to 0.509)
Tumor type (HCC) on V2/F ^c	0.521	29.9	0.521 (0.316 to 0.675)
Tumor type (GBM) on V2/F ^c	0.480	36.9	0.480 (0.221 to 0.704)
Tumor type (MM) on V2/F ^c	0.682	86.4	0.662 (0.389 to 0.870)
Tumor type (brain cancer) on V2/F ^c	0.415	56.1	0.415 (0.019 to 1.04)
Random Effects			
Interindividual variability			
CV%, CL/F	52.2%	14.4	0.261 (0.168 to 0.308)
CV%, V2/F	26.1%	31.5	0.068 (0.029 to 0.097)
CV%, Ka	143.2%	32.3	2.05 (1.60 to 2.75)
CV%, Q	98.1%	33.5	0.962 (0.145 to 1.50)
Residual Variability			
σ^2 (Log additive)	0.092	10.3	0.092 (0.069 to 0.113)

Notes: ^aBootstrap confidence interval values are taken from bootstrap calculation (978 successful out of a total of 1000 bootstrap replicates).

^b $\frac{CL}{F}(L/h) = 3.63 * (1 + 0.007 * (CLcr - 94.42)) * (1 - 0.647)(ifDLBCL) * (1 - 0.692)(ifPCNSL) * (1 - 0.364)(ifOtherSolidTumor) * (1 + 0.309)(ifMM)$.

^c $\frac{V2}{F}(L) = 36.2 * (1 + 0.009 * (BW - 74.5)) * (1 - 0.179)(iffemale) * (1 + 0.476)(ifDLBCL) * (1 + 0.846)(ifPCNSL) * (1 + 0.344)(ifNHL) * (1 + 0.521)(ifHCC) * (1 + 0.480)(ifGBM) * (1 + 0.682)(ifMM) * (1 + 0.415)(ifBrainCancer)$

Abbreviations: ALAG, absorption lag time; CI, confidence interval; CL/F, apparent clearance; Ka, absorption rate constant; Q/F, apparent intercompartmental clearance; TV, typical value; V2/F, apparent volume of distribution of central compartment; V3/F, apparent volume of distribution of peripheral compartment; CLcr, creatinine clearance; DLBCL, diffuse large B cell lymphoma; PCNSL, primary CNS lymphoma; NHL, non-Hodgkin lymphoma; HCC, hepatocellular carcinoma; GBM, glioblastoma multiforme; MM, multiple myeloma; CV%, coefficient of variation; %RSE, relative standard error.

significant covariates on apparent clearance (CL/F). Body weight, sex and tumor types were found statistically significant on apparent central volume of distribution (V2/F).

Tumor types were found to exert distinct effects on CL/F (Figures 1A and 4A). To find out the likely reason of tumor types on CL/F, we conducted a series of analyses based on the PK properties of CC-122. Since the clearance of CC-122 was associated with renal route,⁹ we firstly investigated whether tumor patients had renal deficiencies because literatures have revealed that tumor patients (eg,

MM) were seen with renal failure.^{11,12} However, analyses showed that overall tumor patients showed no obvious difference with regard to renal function (CLcr) compared to healthy subjects (Figure 7A), suggesting that renal function may not play a role here.

Next, we examined the CC-122 metabolic profile. In vitro study has indicated that cytochrome P450 (CYP) 3A and CYP1A2 appear to be the major enzymes involved in the oxidative metabolism of CC-122. Ogasawara et al reported that following co-administering with CYP3A and

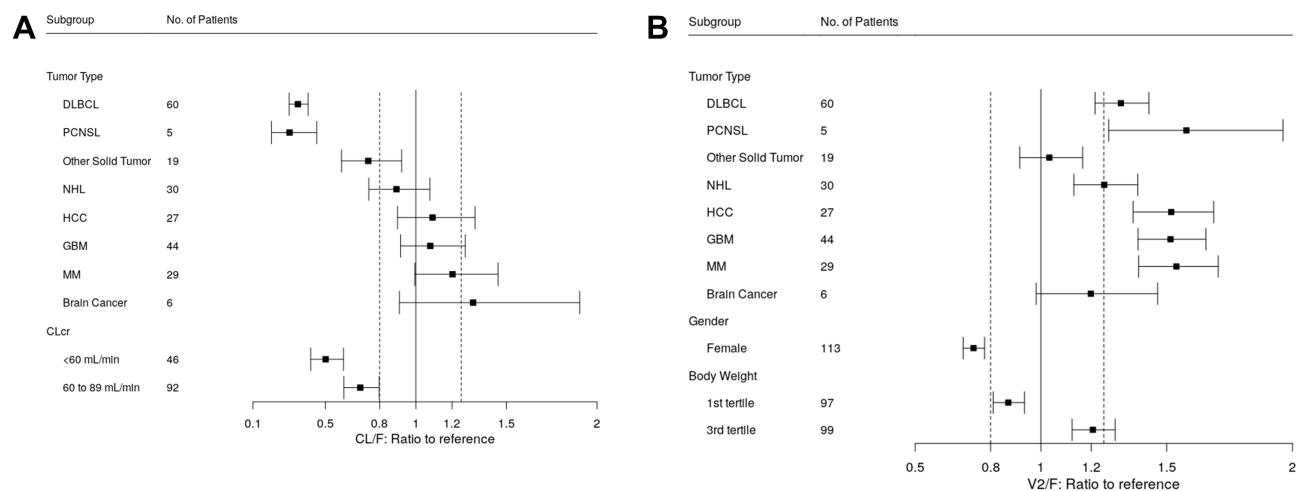


Figure 4 Forest plot of significant covariates on apparent clearance (CL/F, **A**) and apparent volume of distribution of the central compartment (V2/F, **B**) of CC-122. Data are shown as median (90% confidence interval). (**A**) References are healthy subject (tumor type) and creatinine clearance (CLcr) ≥ 90 mL/min (CLcr). (**B**) References are healthy subject (tumor type), male (gender) and second tertile of body weight at baseline (Body weight). First, second and third tertile of body weight at baseline are 39.8–68.0 kg, 68.2–81.6 kg and 81.9–159.0 kg, respectively.

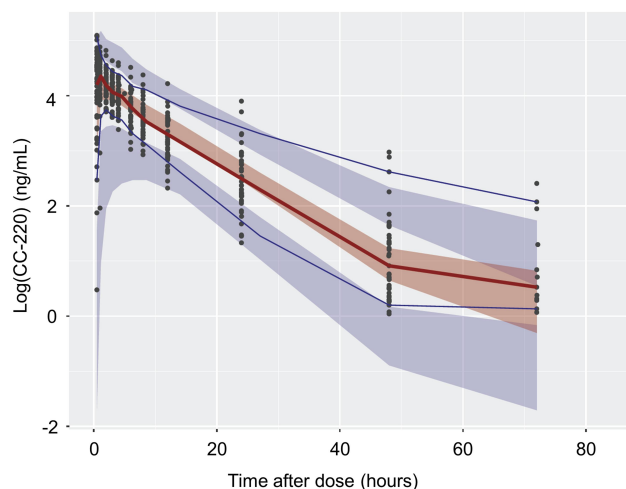


Figure 5 Visual predictive check for plasma CC-122 concentration (log transform) vs time profiles. Circles represent observed data. Lines represent the 5th (solid blue), 50th (solid red), and 95th (solid blue) percentiles of the observed data. Shaded areas represent nonparametric 90% confidence intervals about the 5th (blue), 50th (red), and 95th (blue) percentiles for the corresponding model-predicted percentiles.

CYP1A2 modulators, the exposure and clearance of CC-122 were altered.⁸ Therefore, it was reasonable to investigate the major enzyme activities among tumor patients and non-tumor subjects. However, with a lack of specific enzyme expression data, we used liver function indices (eg, AST, ALT, bilirubin) to represent the overall hepatic activities. By graphical examination, except for HCC (liver cancer), other tumors had comparable AST, ALT and bilirubin levels as compared to non-tumor patients (Figure 7B–D). Given that HCC is a liver cancer, it was not surprising to observe a decrease in liver function. In fact, it has been reported that CYP enzyme activities were down regulated in

tumor tissue samples (eg HCC),^{13–15} which was the major enzyme to metabolize CC-122. However, in contrast to the above observation, HCC patients showed slightly higher CL/F (9%) as compared to healthy subjects though reduced liver function was anticipated, suggesting the existence of other confounding factors rather than liver functions. For other tumor types, no discernible difference was identified with regard to liver functions. However, this interpretation needs to be cautious because liver function indices (eg AST, ALT, bilirubin) may not accurately represent actual CYP enzyme activities. More data are needed to precisely address this hypothesis.

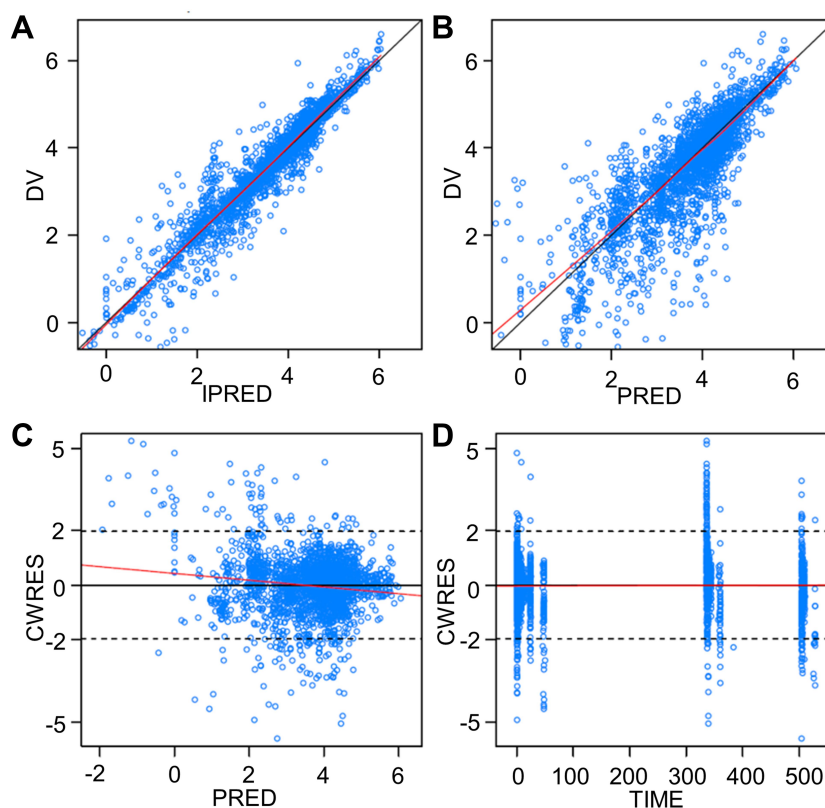


Figure 6 Goodness-of-fit plots of the final population pharmacokinetic model of CC-122. The black line represents the identity line or zero line. The red line represents the locally weighted scatterplot smoothing line. **(A)** Observed concentration vs individual predicted concentration. **(B)** Observed concentration vs population predicted concentration. **(C)** Conditional weighted residual vs population predictions. **(D)** Conditional weighted residual vs time.

Abbreviations: CWRES, conditional weighted residuals; DV, observed value; IPRED, individual predicted values; PRED, predicted values; TIME, time after first dose (hour).

Noteworthy, the multiple pretreat regimens in cancer patients which possibly include the concomitant use of CYP enzyme modulators may also play a role here. However, the lack of data prevented further analysis to be conducted. Notably, the impact of tumor on clearance was also reported in other compounds, including cabozantinib¹⁶ and fedratinib.¹⁷ From these publications, the authors examined multiple relevant factors but failed to identify an exact cause due to the comorbid nature of tumor patients and lack of adequate information.

Renal clearance was known to be one of the major elimination routes for CC-122. From a renal impairment clinical study,⁹ Li et al showed that following administration of a single oral dose of 3 mg CC-122, renal impairment reduced the apparent total plasma clearance and increased the exposure in subjects with mild, moderate, and severe renal insufficiency compared to normal renal function, respectively. In line with the above finding, we herein showed that creatine clearance (CL_{cr}) was strongly correlated with CL/F (Figures 1C and 4A).

Tumor type was found to be correlated with apparent volume of distribution (V₂/F) (Figures 1B and 4B). V₂/F was associated with drug distribution. These data potentially suggested that effect of disease may lead to deeper tissue/organ distribution of the drug, which was consistent with the drug's action on tumor cells. Similar observation was seen in pomalidomide.¹⁰

Body weight (a range from 39.8 to 159.0 kg) was identified as a statistical covariate on V₂/F. Physiologically, increasing body weight was postulated to be in parallel with increasing extracellular fluids,¹⁷ the space where CC-122 was likely to distribute into through diffusion. However, further examination of the forest plot (Figure 4B) indicated that the magnitude of body weight on V₂/F changes were within $\pm 30\%$ of reference cohort. Given the minimal effect, body weight was unlikely to exert any clinical relevance to CC-122.

Sex was found to impact V₂/F (Figures 1E and 4B). There are many possible reasons for sex differences, such as gastric pH and protein binding,^{18,19} which may partly explain the finding. The resulting difference of V₂/F

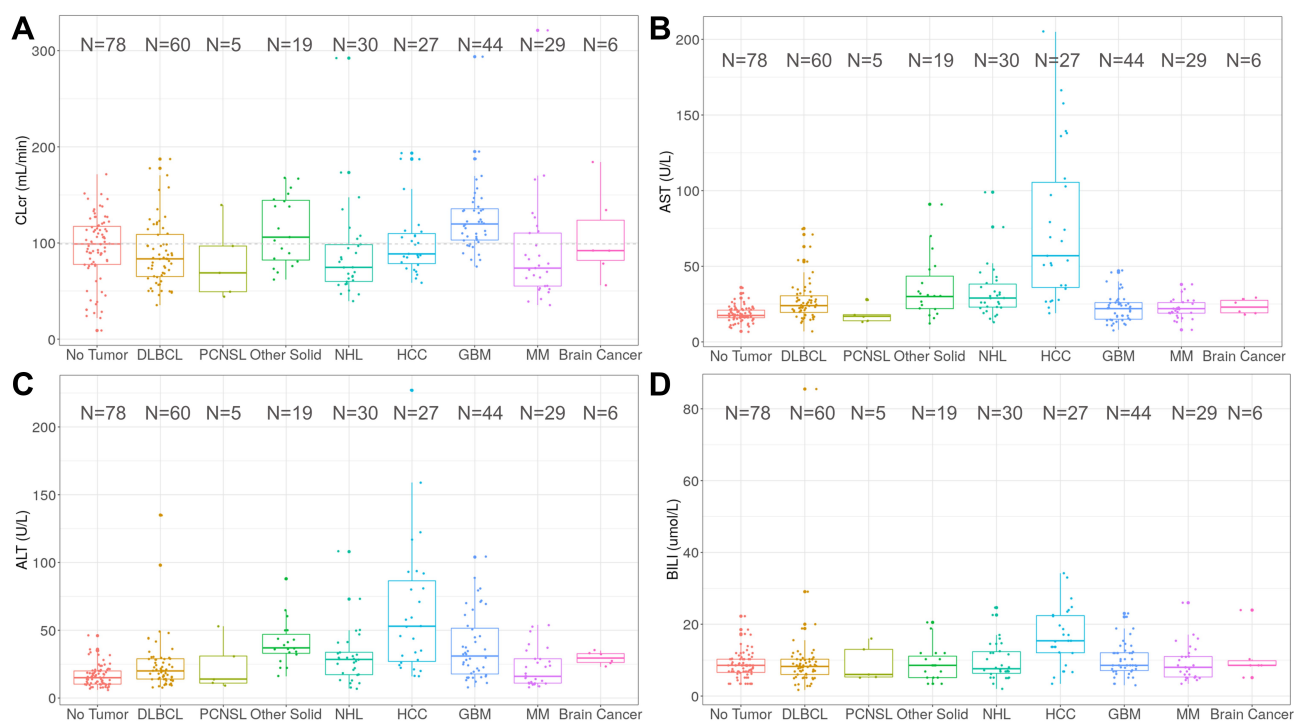


Figure 7 Box plot of baseline creatinine clearance (CLcr, **A**) aspartate aminotransferase (AST, **B**) alanine aminotransferase (ALT, **C**) and bilirubin (BILI, **D**) by tumor types. The number of subjects were presented.

Abbreviations: DLBCL, diffuse large B cell lymphoma; PCNSL, primary CNS lymphoma; other ST, other solid tumor; NHL, non-Hodgkin lymphoma; HCC, hepatocellular carcinoma; GBM, glioblastoma multiforme; MM, multiple myeloma.

between male and female was small (<30%) and therefore this finding was not considered to be clinically significant.

In summary, PK of CC-122 in non-tumor subjects and patients with advanced solid tumors, NHL, MM, or advanced unresectable solid tumors was adequately characterized by a two-compartment model with first-order absorption incorporating a lag time and first-order elimination model. The tumor types had significant effect on CL/F and V2/F. Creatinine clearance was a statistically significant covariate on CL/F. Body weight and sex were statistically but not clinically relevant covariates on V2/F. No other clinically meaningful covariates were identified. Based upon the above analyses, patients with renal deficiency may warrant dose adjustment as compared to normal renal function patients. In addition, the indication-specific PK property findings are likely to inform further clinical development of CC-122 with regard to dose selection.

Data Sharing Statement

The datasets are available from the corresponding author upon request.

Consent for Publication

All the authors have reviewed and concurred with the manuscript.

Acknowledgments

The authors thank all study participants, their families and clinical study team members.

Author Contributions

Y.L. and M.P. contributed to conception and design; J.C. and Y.L. contributed to acquisition of data; Y.C., S.Z. and Y.L. contributed to analysis; M.P. conducted all clinical trials; all authors contributed to interpretation of data; Y.C., S.Z. and Y.L. drafted and revised the article. All authors made substantial contributions to conception and design, acquisition of data, or analysis and interpretation of data; took part in drafting the article or revising it critically for important intellectual content; agreed to submit to the current journal; gave final approval of the version to be published; and agreed to be accountable for all aspects of the work.

Funding

This work was sponsored and funded by Bristol Myers Squibb.

Disclosure

Y.C., J.C., M.P., S.Z. and Y.L. are employees and hold equity ownership in Bristol Myers Squibb. The authors report no other conflicts of interest in this work.

References

- Cubillos-Zapata C, Cordoba R, Avendaño-Ortiz J, et al. CC-122 immunomodulatory effects in refractory patients with diffuse large B-cell lymphoma. *Oncoimmunology*. 2016;5(12):e1231290. doi:10.1080/2162402X.2016.1231290
- Tomimaru Y, Aihara A, Wands JR, Aloman C, Kim M. A novel drug, CC-122, inhibits tumor growth in hepatocellular carcinoma through downregulation of an oncogenic TCF-4 isoform. *Transl Oncol*. 2019;12(10):1345–1356. doi:10.1016/j.tranon.2019.07.002
- Camicia R, Winkler HC, Hassa PO. Novel drug targets for personalized precision medicine in relapsed/refractory diffuse large B-cell lymphoma: a comprehensive review. *Mol Cancer*. 2015;14:207.
- Rasco DW, Papadopoulos KP, Pourdehnad M, et al. A first-in-human study of novel cereblon modulator avadomide (CC-122) in advanced malignancies. *Clin Cancer Res*. 2019;25(1):90–98. doi:10.1158/1078-0432.CCR-18-1203
- Hatake K, Chou T, Doi T, et al. Phase I, multicenter, dose-escalation study of avadomide in adult Japanese patients with advanced malignancies. *Cancer Sci*. 2021;112(1):331–338. doi:10.1111/cas.14704
- Michot JM, Bouabdallah R, Vitolo U, et al. Avadomide plus obinutuzumab in patients with relapsed or refractory B-cell non-Hodgkin lymphoma (CC-122-NHL-001): a multicentre, dose escalation and expansion phase 1 study. *Lancet Haematol*. 2020;7(9):e649–e659. doi:10.1016/S2352-3026(20)30208-8
- Li Y, Carayannopoulos LN, Thomas M, Palmisano M, Zhou S. Exposure-response analysis to assess the concentration-QTc relationship of CC-122. *Clin Pharmacol*. 2016;8:117–125. doi:10.2147/CPAA.S111867
- Ogasawara K, MacGorman K, Liu L, et al. Drug-Drug Interaction Study to assess the effect of cytochrome P450 inhibition and induction on the pharmacokinetics of the novel cereblon modulator avadomide (CC-122) in healthy adult subjects. *J Clin Pharmacol*. 2019;59(12):1620–1631. doi:10.1002/jcph.1453
- Li Y, MacGorman K, Liu L, et al. Single-dose pharmacokinetics, safety, and tolerability of avadomide (CC-122) in subjects with mild, moderate, or severe renal impairment. *Clin Pharmacol Drug Dev*. 2020;9(7):785–796. doi:10.1002/cpdd.760
- Li Y, Xu Y, Liu L, Wang X, Palmisano M, Zhou S. Population pharmacokinetics of pomalidomide. *J Clin Pharmacol*. 2015;55(5):563–572. doi:10.1002/jcph.455
- Dimopoulos MA, Kastritis E, Rosinol L, Bladé J, Ludwig H. Pathogenesis and treatment of renal failure in multiple myeloma. *Leukemia*. 2008;22(8):1485–1493. doi:10.1038/leu.2008.131
- Humphreys BD, Soiffer RJ, Magee CC. Renal failure associated with cancer and its treatment: an update. *J Am Soc Nephrol*. 2005;16(1):151–161. doi:10.1681/ASN.2004100843
- Zhou J, Wen Q, Li SF, et al. Significant change of cytochrome P450s activities in patients with hepatocellular carcinoma. *Oncotarget*. 2016;7(31):50612–50623. doi:10.18632/oncotarget.9437
- Robertson GR, Liddle C, Clarke SJ. Inflammation and altered drug clearance in cancer: transcriptional repression of a human CYP3A4 transgene in tumor-bearing mice. *Clin Pharmacol Ther*. 2008;83(6):894–897. doi:10.1038/clpt.2008.55
- Yan T, Lu L, Xie C, et al. Severely impaired and dysregulated cytochrome P450 expression and activities in hepatocellular carcinoma: implications for personalized treatment in patients. *Mol Cancer Ther*. 2015;14(12):2874–2886. doi:10.1158/1535-7163.MCT-15-0274
- Lacy S, Yang B, Nielsen J, Miles D, Nguyen L, Huttmacher M. A population pharmacokinetic model of cabozantinib in healthy volunteers and patients with various cancer types. *Cancer Chemother Pharmacol*. 2018;81(6):1071–1082. doi:10.1007/s00280-018-3581-0
- Ogasawara K, Zhou S, Krishna G, Palmisano M, Li Y. Population pharmacokinetics of fedratinib in patients with myelofibrosis, polycythemia vera, and essential thrombocythemia. *Cancer Chemother Pharmacol*. 2019;84(4):891–898. doi:10.1007/s00280-019-03929-9
- Farkouh A, Riedl T, Gottardi R, Czejka M, Kautzky-Willer A. Sex-related differences in pharmacokinetics and pharmacodynamics of frequently prescribed drugs: a review of the literature. *Adv Ther*. 2020;37(2):644–655. doi:10.1007/s12325-019-01201-3
- Kekki M, Samloff IM, Ihamaäki T, Varis K, Siurala M. Age- and sex-related behaviour of gastric acid secretion at the population level. *Scand J Gastroenterol*. 1982;17(6):737–743. doi:10.3109/00365528209181087

Clinical Pharmacology: Advances and Applications

Dovepress

Publish your work in this journal

Clinical Pharmacology: Advances and Applications is an international, peer-reviewed, open access journal publishing original research, reports, reviews and commentaries on all areas of drug experience in humans. The manuscript management system is completely online and

includes a very quick and fair peer-review system, which is all easy to use. Visit <http://www.dovepress.com/testimonials.php> to read real quotes from published authors.

Submit your manuscript here: <https://www.dovepress.com/clinical-pharmacology-advances-and-applications-journal>